Climate Dynamics (2020) 55:2343–2350
https://doi.org/10.1007/s00382-020-05390-4

Stratospheric radiative feedback limited by the tropospheric influence in global warming

Yuwei Wang[1] · Yi Huang[1]

Received: 24 February 2020 / Accepted: 21 July 2020 / Published online: 30 July 2020

Abstract
Whether the stratospheric radiative feedback amplifies the global warming remains under debate. The stratospheric water vapor (SWV), one of the primary feedbacks in the stratosphere, is argued to be an important contributor to the global warming. On the other hand, the overall stratospheric feedback, which consists of both the SWV feedback and the stratospheric temperature (ST) feedback, does not amount to a significant value. The key to reconciling these seemingly contradictory arguments is to understand the ST change. Here, we develop a method to decompose the ST change and to quantify the decomposed feedbacks. We find that the SWV feedback, which consists of a 0.04 W m^{-2} K^{-1} direct impact on the top-of-the-atmosphere radiation and 0.11 W m^{-2} K^{-1} indirect impact via ST cooling, is offset by a negative ST feedback of − 0.13 W m^{-2} K^{-1} that is radiatively driven by the tropospheric warming. This compensation results in an insignificant overall stratospheric feedback.

1 Introduction

The global surface temperature is warmed by ~ 1.2 K through the direct radiative effect of doubling the CO_2. The CO_2 direct radiative effect subsequently induces other changes known as feedbacks that further amplify the warming by 2.0–4.5 K (Stocker et al. 2013). Although it is well recognized that the rapid adjustment of the stratosphere to CO_2 perturbation adds a significant flux perturbation to the CO_2 radiative forcing (e.g., Zhang and Huang 2014), the radiative impact of stratospheric response to surface warming, i.e., as a feedback mechanism, is less understood.

One prevailing view is that the stratospheric radiative feedback is significant. The stratospheric water vapor (SWV) is argued to be an important contributor to the global warming (Stuber et al. 2001; Forster et al. 2002; Solomon et al. 2010; Dessler et al. 2013; Banerjee et al. 2019). As CO_2 increases, the stratosphere is moistened due to the warming of the tropopause, which suppresses the freezing-drying process (Gettelman et al. 2009; Smalley et al. 2017). An increase in SWV causes both direct and indirect radiative perturbations (RPs) at TOA. It immediately reduces the outgoing longwave radiation (OLR), leading to a direct RP, and also cools the stratosphere which further reduces the OLR, leading to an indirect RP. The SWV feedback, which consists of both the direct and indirect RPs, is estimated to be 0.18 ± 0.05 W m^{-2} K^{-1} (global mean radiation flux change per degree of surface warming) in the global climate models (GCMs) of the Coupled Model Intercomparison Project 5 (CMIP5) (Banerjee et al. 2019).

However, contrary to the prevailing view that is centered on the SWV perspective, it is also found that the overall stratospheric feedback, which consists of both the SWV feedback and the stratospheric temperature (ST) feedback, is negligibly small (Huang et al. 2016, 2020). The overall TOA radiative flux change is estimated to be 0.00 ± 0.05 W m^{-2} K^{-1} in the GCMs of CMIP5, using the kernel method (Huang et al. 2016).

The key to reconciling the contradiction is to understand the ST change. As alluded by the previous research (Huang et al. 2016; Banerjee et al 2019), a GCM-simulated ST change in the global warming simulation is not only driven by the SWV. Here, we aim to understand how the overall feedback response in ST arises and why it differs from the SWV-driven change. We present a novel method

Electronic supplementary material The online version of this article (https://doi.org/10.1007/s00382-020-05390-4) contains supplementary material, which is available to authorized users.

✉ Yuwei Wang
yuwei.wang@mail.mcgill.ca

1 Department of Atmospheric and Oceanic Sciences, McGill University, 805 Sherbrooke Street West, Montreal, QC H3A 0B9, Canada

for decomposing the overall ST change. With this method, we show that the ST change in the global warming simulation is considerably less than the SWV-induced cooling, because other factors controlling the ST response, such as tropospheric temperature, offset the ST change driven by SWV.

We note that the total stratospheric change in response to the CO_2 increase can be decomposed into the rapid adjustment responses and slow feedback responses. The responses concerned here are the feedback responses associated with surface warming, while the responses directly driven by CO_2 radiative forcing, i.e., the forcing adjustment, are included in supplementary material for a comparison.

2 Method and model description

2.1 Diagnostic method

The overall ST change as a feedback response is decomposed as:

$$\Delta ST \cong \Delta ST_{stra\_wv} + \Delta ST_{stra\_dyn} + \Delta ST_{trop\_T} + \Delta ST_{trop\_wv} + \Delta ST_{cld} + \Delta ST_{surf\_T} + \Delta ST_{surf\_alb} \tag{1}$$

ΔST is the overall ST change in response to the surface warming. ΔST_{stra_wv} is the radiative temperature adjustment to the SWV perturbation. Other terms on the right-hand side of the equation are radiative temperature adjustments to various perturbations. The perturbations decomposed here are: stratospheric dynamics (stra_dyn), tropospheric temperature (trop_T), tropospheric water vapor (trop_wv), cloud (cld), surface temperature (surf_T), and surface albedo (surf_alb). The theoretical basis of the decomposition is described in the Appendix.

Based on Eq. (1), the ST feedback parameter can be decomposed as:

$$\lambda_{ST} \cong \lambda_{ST\_stra\_wv} + \lambda_{ST\_stra\_dyn} + \lambda_{ST\_trop\_wv} + \lambda_{ST\_trop\_T} + \lambda_{ST\_cld} + \lambda_{ST\_surf\_T} + \lambda_{ST\_surf\_alb} \tag{2}$$

Each of the components is the feedback parameter of the ST change driven by a specific perturbation, evaluated as $\lambda_X = \Delta R_X / \Delta T_S$. ΔR_X is the radiative flux change at the TOA and is measured by running an offline radiative transfer model (PORT) with and without the ST adjustment to the perturbation. ΔT_S equals 4.5 K, as given by a GCM experiment (see below).

2.2 GCM set up

The GCM model used here is CAM4 (Neale et al. 2010), which is the atmospheric component of Community Climate System Model version 4 (CCSM4) that participated in CMIP5. The dynamical scheme is Finite Volume, with a $1.9° \times 2.5°$ horizontal resolution, and 30 vertical levels with the model top at around 3 hPa. The physical parameterization schemes are set as the default settings. The radiation scheme is CAMRT, the shallow convection is the Hack scheme and the deep convection is the Zhang-McFarlane scheme. The CO_2 concentration is fixed to 1468 ppmv ($4 \times CO_2$). The prescribed SST and sea ice concentrations are generated from the monthly mean data of the last 30 years (out of 1300 years) in the CCSM4 piControl experiment and the last 10 years (out of 150 years) in the CCSM4 abrupt $4 \times CO_2$ experiment from CMIP5.

Three types of experiments, as defined in CMIP5 (Taylor et al. 2012), are used in this paper: piControl, sstclim $4 \times CO_2$, and abrupt $4 \times CO_2$. The piControl and the abrupt $4 \times CO_2$ experiments are conducted using coupled AOGCMs forced by $1 \times CO_2$ and $4 \times CO_2$ respectively. The sstclim $4 \times CO_2$ experiment is a $4xCO_2$ atmosphere-only simulation prescribed with the SST from the piControl experiment.

We first conduct a CAM4 control experiment, which is run for 30 years with prescribed SST from CCSM4 piControl experiment. This is to mimic the CMIP5 sstclim $4 \times CO_2$ experiment. This control run outputs the radiation-related variables, including the temperature profile, water vapor distribution, surface albedo, clouds, and the dynamical heating rate, at each model integration time step (30 min) for 2 years. Then we conduct a perturbed run, which is similar to the control run but prescribed with SST from CCSM4 abrupt $4 \times CO_2$ experiment. The output of atmospheric profiles from the two runs is then used to drive the offline radiative transfer model (see below).

2.3 Radiative transfer experiments

For the radiative flux computation, we follow Banerjee et al. (2019) and take advantage of the parallel offline radiative transfer (PORT) model (Conley et al. 2013). It utilizes the CAM4 framework but only performs the radiative transfer calculation. Using the same framework as CAM4, PORT is able to reproduce the same heating rates and LW and SW fluxes as those in CAM4. Furthermore, PORT is also capable of performing radiative adjustment in the stratosphere, following the idea of fixed dynamical heating (Ramanathan and Dickson 1979; Fels et al. 1980).

Taking the SWV perturbation as an example, we explain the experimental procedure in the following. The purpose of the experiment is to identify, through an iterative procedure, the stratospheric temperature change that can compensate the radiative heating rate change imposed by the SWV change. The radiative heating rate perturbation imposed by the SWV change is calculated by the following equation:

$$\left(\frac{dST}{dt}\right)_i = H(ST_i, X + \Delta X) - H(ST_0, X) \quad (3)$$

Here ΔX is the change of the SWV. ST_0 is the original stratospheric temperature and ST_i is the stratospheric temperature at the ith iteration step. Hence the stratospheric temperature at the next time step is obtained by adding a temperature increment:

$$ST_{i+1} = ST_i + \left(\frac{dST}{dt}\right)_i * \Delta t \quad (4)$$

Here Δt is time step length, which is taken to be 30 min. The integration is repeated until $\frac{dST}{dt}$ is close to zero. More detailed explanations of this method are documented in Wang and Huang (2020). Different from that paper, we only update the temperature in the stratosphere. The same procedure is also applied to the perturbations of tropospheric temperature, tropospheric water vapor, cloud, surface temperature, and surface albedo.

Note that the use of PORT is necessitated in order to obtain the heating rates in Eq. (3) and then, through the iteration procedure, the hypothetical, partial stratospheric temperature change due to respective radiative perturbations, which are not available from CAM run itself. Although approximation methods (e.g., Huang and Wang 2019) can be used to estimate the adjusted stratospheric temperature, the use of a radiation model (PORT) guarantees high accuracy in the results.

To close the decomposition of the ST change, the change of the dynamical heating rate is also taken into consideration. The temperature tendency driven by the stratospheric dynamical heating rate change is computed as:

$$\left(\frac{dST}{dt}\right)_i = H(ST_i, X) - H(ST_0, X) + \Delta H(stra\_dyn) \quad (5)$$

$\Delta H(stra\_dyn)$ is the stratospheric dynamical heating rate difference between the CAM4 perturbed simulation and the control simulation.

Each of the ST feedback components, ΔR_X, is obtained by differencing the TOA radiative fluxes between the PORT simulations with and without radiative temperature adjustment. We spin up PORT for 8 months and then run for another 1 year for the analysis. For example, for the first term $\lambda_{ST\_stra\_wv}$, we first run PORT without ST adjustment to calculate the direct RP, and then run PORT again to calculate the direct RP plus indirect RP by allowing ST to change. The indirect RP induced by the ST change is the TOA flux difference between the second run and the first run. The feedback parameter $\lambda_{ST\_stra\_wv}$ is then obtained by dividing the indirect RP of SWV $\Delta R_{ST\_stra\_wv}$ by the global mean surface temperature change. To account for the feedback dependence on the base climate, we do both the forward and the backward differencing simulations. In the forward method, the perturbation is added to the CAM4 control climate, while in the backward method, the perturbation is subtracted from the CAM4 perturbed climate.

3 Results

Figure 1 illustrates the feedback ST changes associated with the surface warming in the global warming simulations. Figure 1a shows the CMIP5 multi-model mean ST response (see Fig. S2 in Supplementary Material for the response in

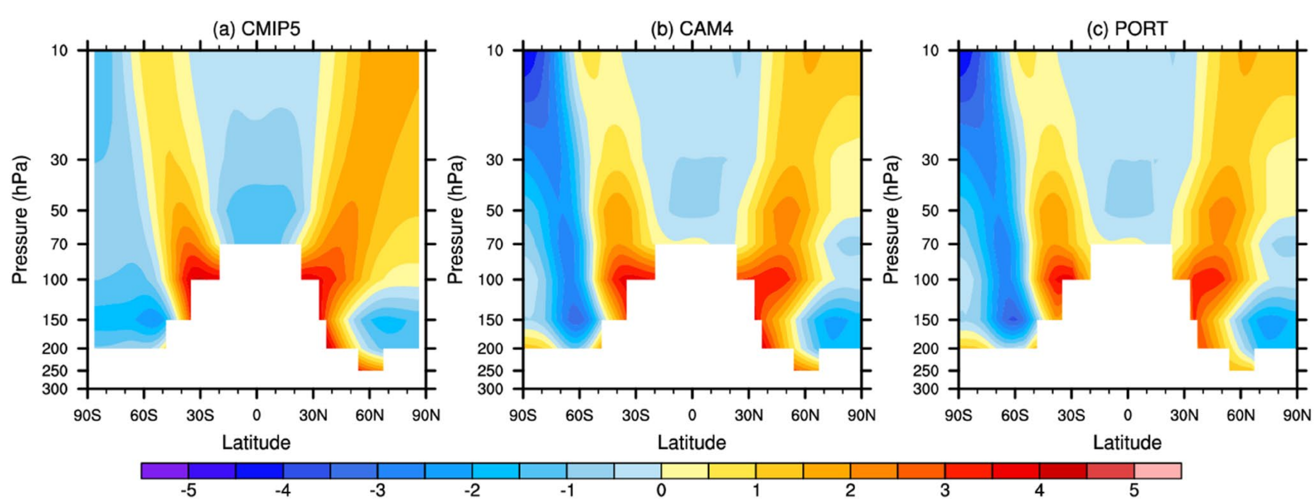

Fig. 1 ST changes in response to the surface warming. **a** Multi-model mean ST response, measured by the difference between the abrupt4xCO_2 experiments and sstclim4×CO_2 experiments of 12 CMIP5 AOGCMs. **b** ST response reproduced by CAM4, measured by the difference between the perturbed experiment and the control experiment. **c** ST response reproduced by PORT in the radiative adjustment experiments. Units: K

individual models). This result is obtained by differencing the ST field in the abrupt4xCO_2 experiment and sstclim $4\times CO_2$ experiment in CMIP5. The change in ST is characterized by the warming in the mid-latitudes and cooling in the tropics and the high-latitudes (Huang et al. 2016). As shown in Fig. 1b, c, this pattern is well captured by CAM4 and PORT.

It is well established that the ST is largely determined by the radiative process (Goody and Yung 1995). We are interested to identify how surface and atmospheric perturbations each radiatively drive the ST change. The perturbations concerned here include changes in SWV, tropospheric temperature, tropospheric water vapor, cloud, surface temperature, and surface albedo (Fig. 2). These perturbations represent the feedback responses of these variables to $4\times CO_2$ global warming and are determined from the differences between the CAM4 perturbed experiment and control experiment.

The SWV increases noticeably, especially in the extratropical lowermost stratosphere, resembling what was found previously (Dessler et al. 2013; Banerjee et al. 2019). The tropospheric water vapor also increases and the pattern is characterized by the enhanced moistening in the tropical upper troposphere and polar lower troposphere and corresponds to the amplified warming in these regions. The surface albedo shows two strong declines in the Arctic and the Southern Ocean (around 60°S), where large fractions of sea ice have melted. Moreover, a robust stratospheric circulation change is the acceleration of the Brewer–Dobson circulation (BDC), as reflected by the increases in both updraft speed in the ascending branch of BDC in the tropics and downdraft speed in the descending branch in the mid-latitudes (Garcia and Randel 2008). Cloud changes are characterized by generally elevated high clouds in accordance with the increase of the depth of the tropospheric circulation (Thompson et al. 2017).

The radiative adjustments of ST driven by each of the above changes are shown in Fig. 3. In general, both the SWV increase and the tropospheric water vapor increase act to cool the stratosphere, while the warming of the troposphere and the warming of the surface act to warm the stratosphere. The albedo change only has a small effect on ST. The circulation and the cloud changes induce alternating patterns in ST changes. The small residual confirms the closure of the ST decomposition (see more discussion in the "Appendix").

The increase in SWV significantly cools the whole stratosphere (Fig. 3a), in accordance with the previous studies (Stuber et al. 2001; Forster et al. 2002; Solomon et al. 2010; Dessler et al. 2013; Banerjee et al. 2019). The cooling is the

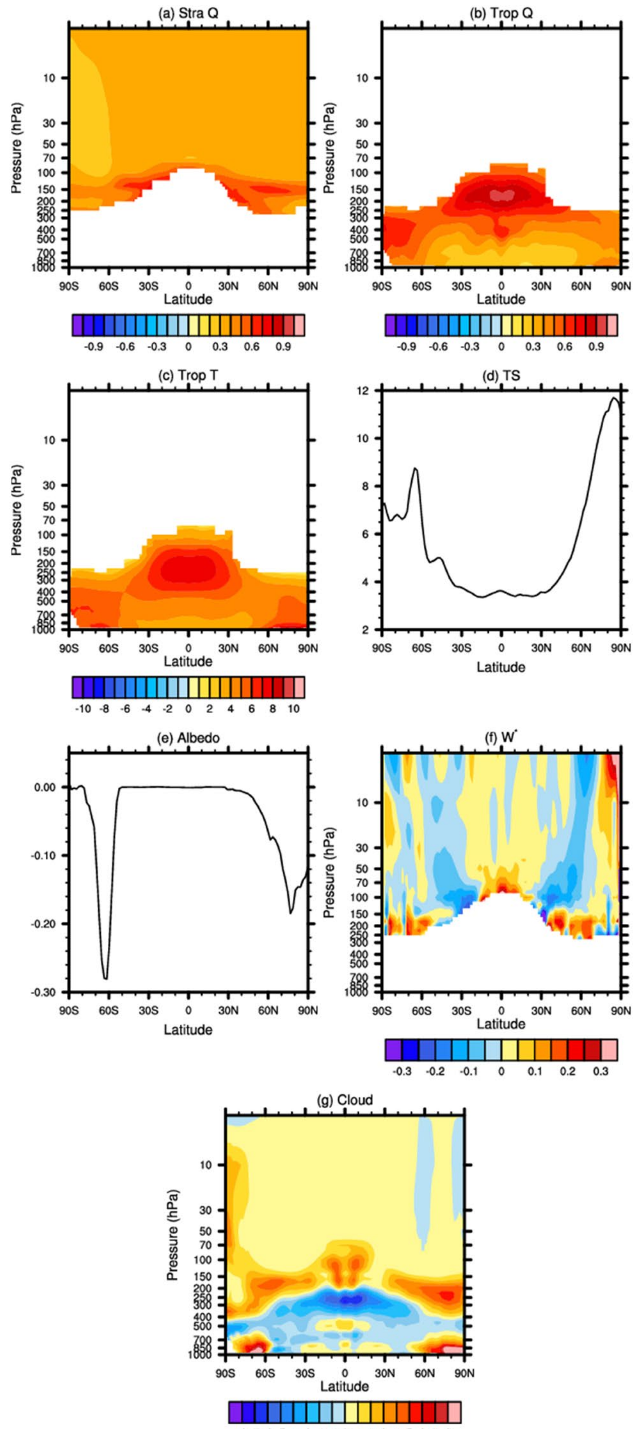

Fig. 2 Feedback climate changes simulated by CAM4, by differencing the CAM4 perturbed experiment and the control experiment. Shown in order are the changes in (A) the logarithm of specific humidity $\Delta\ln(q)$ in stratosphere, **b** $\Delta\ln(q)$ in troposphere, **c** tropospheric temperature (K), **d** surface temperature (K), **e** surface albedo, **f** vertical velocity of the residual circulation (mm s^{-1}), and **g** cloud fraction (%)

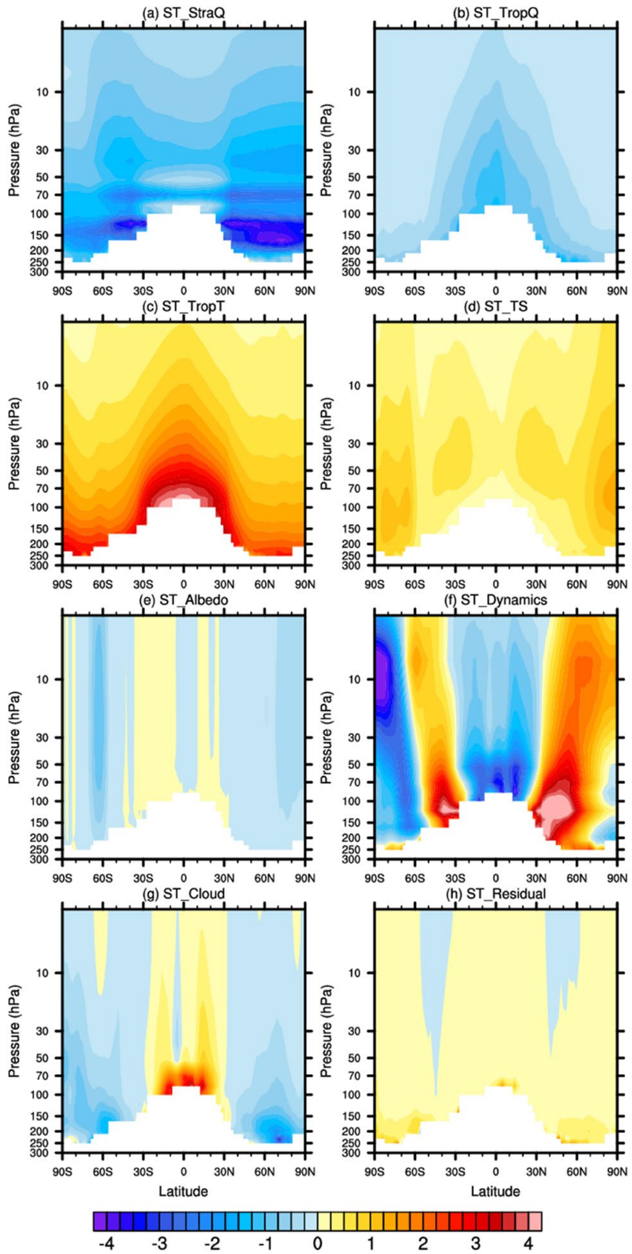

Fig. 3 PORT-simulated ST change driven by different perturbations: **a** SWV, **b** tropospheric water vapor, **c** tropospheric temperature, **d** surface temperature, **e** surface albedo, **f** stratospheric dynamical heating rate, and **g** cloud. The residual **h** is the temperature difference between the ST change in CAM4 and the sum of the perturbation-driven ST changes (**a**–**g**). The results shown here are the average of the forward and backward differencing simulations. Units: K

largest in the extra-tropical lowermost stratosphere where the water vapor increases the most. The cooling is because SWV increases the stratospheric emissivity, resulting in more longwave (LW) radiation emitting to the space and to the troposphere. Although the absorptivity increase in the shortwave (SW) band also leads to enhanced absorption of the solar flux, the SW effect is much weaker than the LW effect (see Sect. 3 in Supplementary Material). The cooling pattern discloses two minima between 50 and 100 hPa, especially in the tropical region. This feature is probably because of the non-uniform distribution of the water vapor change and the temperature inversion in the stratosphere (Fig. S4). The increased tropospheric water vapor also cools the stratosphere (Fig. 3b) due to the enhanced absorption of LW radiation, which effectively reduces the amount of radiation that stratosphere receives from the underlying troposphere and the surface.

However, the warming of the troposphere leads to a significant warming in the stratosphere (Fig. 3c). This effect is strong especially in the tropical and polar regions, corresponding to the underlying tropospheric warming centers. The tropospheric warming increases the amount of thermal radiation (the Planck effect) emitted from the troposphere to the stratosphere and causes the stratosphere to warm (Lin et al. 2017). For the same reason, surface warming also warms the stratosphere, although to a lesser extent (Fig. 3d). The surface temperature effect reaches a maximum where the troposphere is dry, allowing most surface radiation to reach the stratosphere.

The surface albedo change only induces a slight cooling in the stratosphere (Fig. 3e), a consequence of melting sea ice which reduces the reflected shortwave (SW) radiation back to the stratosphere.

The temperature change driven by the BDC acceleration discloses a bullhorn-shaped pattern (Fig. 3f), with cooling in the ascending branch and warming in the descending branch, as found by Huang et al. (2016). This effect shows a strong heterogeneity. Although the magnitudes of the temperature change are locally strong, the global mean effect on the radiation budget is small due to the offsetting effects from different regions.

Cloud change induces warming in the tropics and cooling in the extra-tropics (Fig. 3g). The high clouds have a strong greenhouse effect and reduce the LW radiation to the stratosphere. The tropical high clouds show a decrease in emissivity (absorptivity) below 100 hPa, which facilitates more thermal radiation from the troposphere into the stratosphere. The emissivity increase at 70 hPa in the tropical stratosphere enhances the warming in the lower tropical stratosphere (Fig. S5 in Supplementary Material). The extra-tropical cooling is due to the significant increase in the emissivity of the extra-tropical high cloud, especially in the wintertime.

Each of the ST changes shown in Fig. 3 leads to the radiation flux change at the TOA. Table 1 lists the values of flux

Table 1 Decomposition of stratospheric feedbacks

	SWV	ST	ST_StraQ	ST_TropQ	ST_TropT	ST_TS	ST_Albedo	ST_Dyn	ST_Cloud	ST_Res
Forward method										
Flux changes at TOA (W m^{-2})	0.23	−0.13	0.53	0.19	−0.56	−0.18	0.03	−0.21	0.17	−0.08
Feedbacks (W m^{-2} K^{-1})	0.05	−0.03	0.12	0.04	−0.12	−0.04	0.01	−0.05	0.04	−0.02
Backward method										
Flux changes at TOA (W m^{-2})	0.11	−0.08	0.51	0.21	−0.65	−0.14	0.03	−0.18	−0.09	0.23
Feedbacks (W m^{-2} K^{-1})	0.03	−0.02	0.11	0.05	−0.14	−0.03	0.01	−0.04	−0.02	0.05
Average										
Feedbacks (W m^{-2} K^{-1})	0.04	−0.02	0.11	0.04	−0.13	−0.04	0.01	−0.04	0.01	0.02

changes and the associated feedbacks. The feedbacks are measured by dividing the global mean flux changes by the global mean surface temperature change (4.5 K). The results include both the forward and backward simulations. The following discussion is based on their average.

The stratospheric feedback consists of the SWV feedback and the ST feedback. The direct radiative effect of SWV is 0.04 W m^{-2} K^{-1} and the overall effect of ST change is − 0.02 W m^{-2} K^{-1}, which are considerably smaller than the tropospheric feedbacks. The decomposition of the ST change shows that the significant positive ST feedback driven by the SWV increase (ST_StraQ) is offset by the negative ST feedback of similar magnitude caused by the tropospheric temperature increase (ST_TropT). The ST_StraQ feedback is 0.11 W m^{-2} K^{-1} while the ST_TropT feedback is − 0.13 W m^{-2} K^{-1}. The sum of the SWV direct effect and the indirect effect via ST_StraQ is 0.15 W m^{-2} K^{-1}, close to 0.18 W m^{-2} K^{-1} estimated from CMIP5 multi-model ensemble (Banerjee et al. 2019). Other ST feedback components are all much smaller in terms of the global mean being less than or equal to 0.04 W m^{-2} K^{-1} in magnitude. The result suggests the radiative impact of tropospheric warming on the stratosphere limits the stratospheric radiative feedback.

4 Conclusions

In conclusion, to better understand the ST change and the stratospheric radiative feedback in global warming, a novel method is developed here to decompose the overall ST feedback to seven components. Our results affirm that the overall stratospheric feedback is small, as a result of offsetting component feedbacks. The most notable offset is between a positive SWV feedback consisting of both direct and indirect radiative effects of SWV and a negative feedback of ST due to the tropospheric warming.

Acknowledgements We acknowledge a grant from the Natural Sciences and Engineering Research Council of Canada (RGPIN-2019-04511) that supported this research. YW acknowledges the support of the McGill Space Institute Postdoctoral Fellowship.

Appendix: Additivity of component ST changes

The closure test presented in the paper (Fig. 3h) verifies the linear additivity of the component ST changes decomposed via the radiative adjustment simulations. Here we present an additional perspective on the validity of the decomposition. Following Huang and Wang (2019), we consider the radiative adjustment process as seeking the atmospheric (stratospheric) temperature change to compensate the radiative heating rate perturbation (HRP) caused by a forcing, X (e.g., SWV or tropospheric temperature perturbation):

$$\Delta H_X + \Delta H_T = 0$$

Here, ΔH_X represents the HRP caused by X and ΔH_T represents the HRP caused by temperature adjustment. As ΔH_T can be well approximated by the temperature Jacobians J,

$$\Delta H_T \approx J_{T,X} \cdot \Delta T$$

the temperature adjustment to the X perturbation can be obtained as,

$\Delta T_X = -J_{T,X}^{-1} \cdot \Delta H_X.$

Each of the seven forcings concerned here has a distinct HRP pattern, which altogether reproduces the overall HRP (Fig. 4). It follows from the above equation that the ST response to each of the forcings can be identified and their sum reproduces the total ST change. We note that the results of the ST decomposition presented in the paper (Fig. 3) are based on the numerical simulation of the radiative adjustment process instead of the Jacobian approximation.

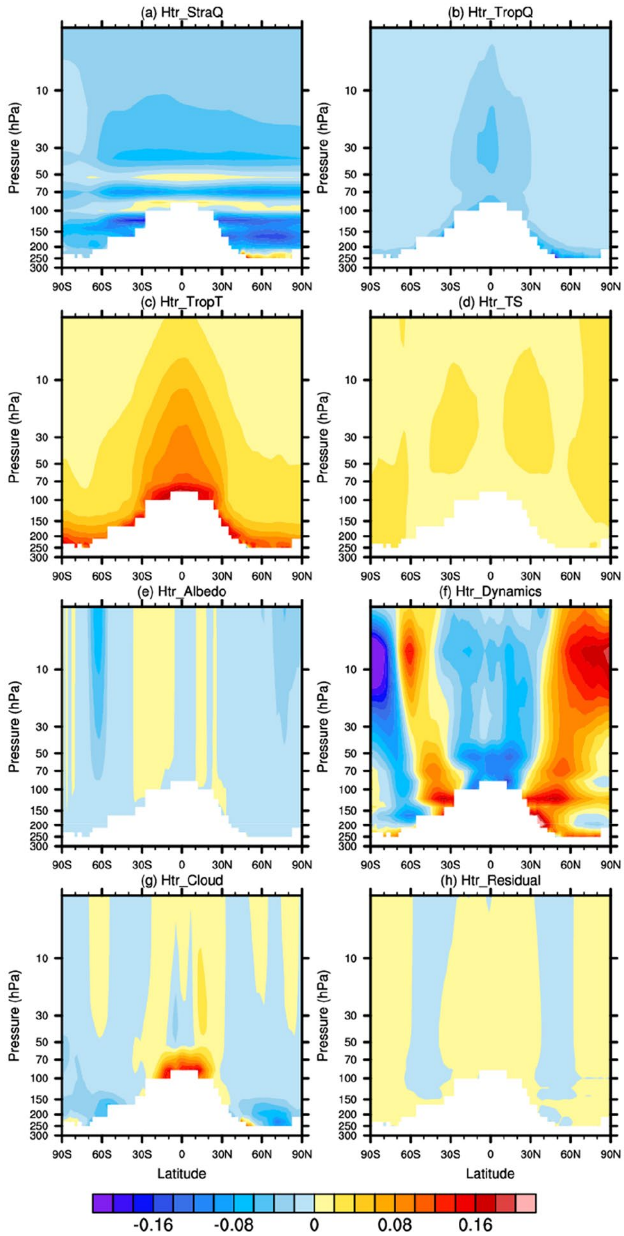

Fig. 4 PORT-simulated stratospheric heating rate changes driven by different perturbations. The heating rate change of each perturbation is obtained by differencing the radiative heating rates simulated by PORT from the atmospheric profiles with and without CAM4 perturbations. Both the forward differencing and the backward differencing methods are conducted using PORT. The results shown here are the average of the two. PORT simulations are based on instantaneous profiles at 30-min intervals. The heating rate changes are averaged over 1 year, the same period as the temperature adjustment simulations shown in Fig. 3. Units: K/day

References

Banerjee A, Chiodo G, Previdi M, Ponater M, Conley AJ, Polvani LM (2019) Stratospheric water vapor: an important climate feedback. Clim Dyn 53(3–4):1697–1710

Conley A, Lamarque J-F, Vitt F, Collins W, Kiehl J (2013) PORT, a CESM tool for the diagnosis of radiative forcing. Geosci Model Dev 6(2):469–476

Dessler A, Schoeberl M, Wang T, Davis S, Rosenlof K (2013) Stratospheric water vapor feedback. Proc Natl Acad Sci 110(45):18087–18091

Fels S, Mahlman J, Schwarzkopf M, Sinclair R (1980) Stratospheric sensitivity to perturbations in ozone and carbon dioxide: radiative and dynamical response. J Atmos Sci 37(10):2265–2297

Forster P MF, Shine K (2002) Assessing the climate impact of trends in stratospheric water vapor. Geophys Res Lett 29(6):10-11–10-14

Garcia RR, Randel WJ (2008) Acceleration of the Brewer–Dobson circulation due to increases in greenhouse gases. J Atmos Sci 65(8):2731–2739

Gettelman A, Birner T, Eyring V, Akiyoshi H, Bekki S, Brühl C, Dameris M, Kinnison DE, Lefèvre F, Lott F (2009) The tropical tropopause layer 1960–2100. Atmos Chem Phys 9(5):1621–1637

Goody RM, Yung YL (1995) Atmospheric radiation: theoretical basis. Oxford University Press, Oxford

Huang Y, Zhang M, Xia Y, Hu Y, Son S-W (2016) Is there a stratospheric radiative feedback in global warming simulations? Clim Dyn 46(1–2):177–186

Huang Y, Wang Y, Huang H (2020) Stratospheric water vapor feedback disclosed by a locking experiment Geophys Res Lett **(in press)**

Huang Y, Wang Y (2019) How does radiation code accuracy matter? J Geophys Res Atmos 124(20):10742–10752

Lin P, Paynter D, Ming Y, Ramaswamy V (2017) Changes of the tropical tropopause layer under global warming. J Clim 30(4):1245–1258

Neale RB et al (2010) Description of the NCAR Community Atmosphere Model (CAM 4.0). NCAR Technical Note NCAR/TN-486+STR, National Center for Atmopsheric Research, Boulder, CO, pp 268

Ramanathan V, Dickinson RE (1979) The role of stratospheric ozone in the zonal and seasonal radiative energy balance of the earth-troposphere system. J Atmos Sci 36(6):1084–1104

Smalley KM, Dessler AE, Bekki S, Deushi M, Marchand M, Morgenstern O, Plummer DA, Shibata K, Yamashita Y, Zeng G (2017) Contribution of different processes to changes in tropical lower-stratospheric water vapor in chemistry–climate models. Atmos Chem Phys 17(13):8031–8044

Solomon S, Rosenlof KH, Portmann RW, Daniel JS, Davis SM, Sanford TJ, Plattner G-K (2010) Contributions of stratospheric water vapor to decadal changes in the rate of global warming. Science 327(5970):1219–1223

Stocker TF, Qin D, Plattner GK, Tignor M, Allen SK, Boschung J, Nauels A, Xia Y, Bex V, Midgley PM (2013) Climate change 2013: The physical science basis. Cambridge University Press, Cambridge

Stuber N, Ponater M, Sausen R (2001) Is the climate sensitivity to ozone perturbations enhanced by stratospheric water vapor feedback? Geophys Res Lett 28(15):2887–2890

Taylor KE, Stouffer RJ, Meehl GA (2012) An overview of CMIP5 and the experiment design. Bull Am Meteor Soc 93(4):485–498

Thompson DW, Bony S, Li Y (2017) Thermodynamic constraint on the depth of the global tropospheric circulation. Proc Natl Acad Sci 114(31):8181–8186

Wang Y, Huang Y (2020) Understanding the atmospheric temperature adjustment to CO2 perturbation at the process level. J Clim 33(3):787–803

Zhang M, Huang Y (2014) Radiative forcing of quadrupling CO2. J Clim 27(7):2496–2508